Dalton Transactions

An international journal of inorganic chemistry

This article can be cited before page numbers have been issued, to do this please use: Z. Zhang, Y. Xiao, M. F. Cui, J. Tang, Z. Fei, L. Qing, X. Chen and X. Qiao, *Dalton Trans.*, 2019, DOI: 10.1039/C9DT03332G.

ROYAL SOCIETY OF CHEMISTRY

rsc.li/dalton

View Article Online
DOI: 10.1039/C9DT03332G

Modulating the basicity of Zn-MOF-74 via cation exchange with calcium-ions

Graphical Abstract

Fine-tuning of the metal-based molecular building blocks in Zn-MOF-74 through post-synthetic cation exchange with Ca^{2+} significantly enhance the basicity and corresponding catalytic performance. The resulting material, exemplified by the Ca/Zn-MOF-74, is shown through Knoevenagel condensation to exhibit improved product yield over parent Zn-MOF-74 and Ni/Zn-MOF-74.

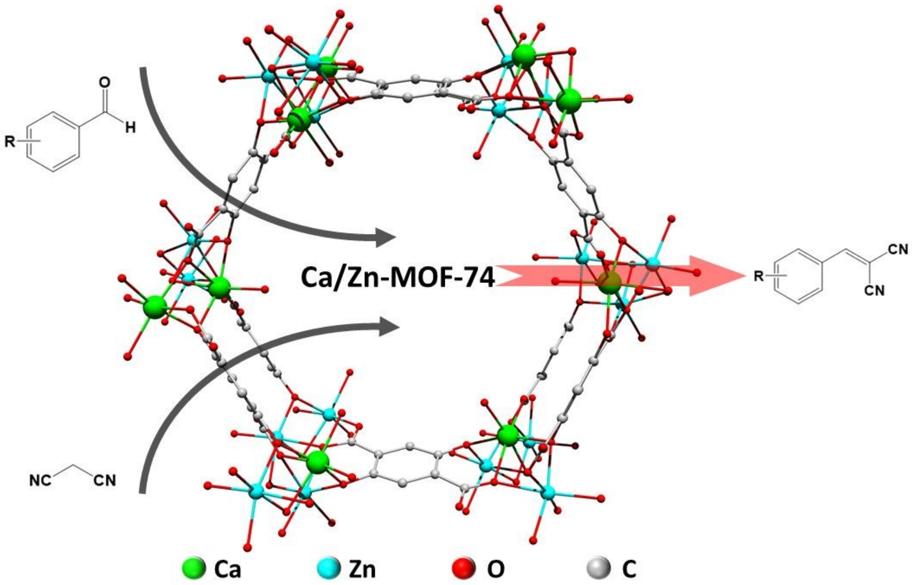

View Article Online
DOI: 10.1039/C9DT03332G

COMMUNICATION

Received 00th January 20xx,
Accepted 00th January 20xx
DOI: 10.1039/x0xx00000x

Modulating the basicity of Zn-MOF-74 via cation exchange with calcium-ions

Zhuxiu Zhang,[a] Yue Xiao,[a] Mifen Cui, [a] Jihai Tang,*[ab] Zhaoyang Fei,[ab] Qing Liu,[a] Xian Chen[a] and Xu Qiao*[ab]

Fine-tuning of the metal-based molecular building blocks in Zn-MOF-74 through post-synthetic cation exchange with Ca^{2+} significantly enhance the basicity and corresponding catalytic performance. The resulting material, exemplified by the Ca/Zn-MOF-74, is shown through Knoevenagel condensation to exhibit improved product yield over parent Zn-MOF-74 and Ni/Zn-MOF-74.

Metal-organic frameworks (MOFs), also knowns as porous coordination polymers (PCPs), have emerged as a new class of crystalline materials with diverse compositions and permanent porosities.[1] The crystal engineering approach[2], in particular the pre-selection[3] or post-synthetic modification[4] of the metal-based molecular building blocks (MBBs), enables the design of MOF structures with target-specific catalytic properties for various reactions.[5] Since the seminal work of Kim[6] and Fujita[7], most studies of MOF catalysts focused upon the Lewis/Brönsted acidity[8] or redox activity[9] of inorganic nodes. MOFs that function as solid base catalysts remains relatively underexplored.[10]

MOFs with intrinsic basicity are exemplified by the way that alkaline earth metal-based MBBs can be incorporated in MOF structures, usually as infinite metal-oxygen/hydroxide chain[11]. The basic site in alkaline earth MOFs is thereby derived from M-O-M species, similar as the low-coordination sites in alkaline earth metal oxides[12]. In this context, Mg-MOF-74 composed of magnesium oxide strand-like MBBs linked by 2,5-dihydroxyterephthalate was found to be an active catalyst in Knoevenagel condensation which is a typical base-catalyzed reaction.[13] Theoretical study reveals that the adsorption of the donor molecule (e.g. malononitrile and ethyl cyanoacetate) on the Mg-O-Mg species in Mg-MOF-74 exhibit lower energy level than other M-MOF-74 iso-structures (M = Ni, Co, Zn). However, it is Ni-MOF-74 rather than Mg-MOF-74 that exhibits best catalytic activity. The critical step of Knoevenagel condensation is the deprotonation of donor molecules, which is highly associated with the proton affinity of phenolate oxygen in M-O-M species.[14] Unfortunately, proton affinity of phenolate oxygen in Mg-MOF-74 is lower than in other M-MOF-74 iso-structures.[13] Given the base strength of alkaline earth metal oxides being in the sequence of BaO > SrO > CaO > MgO, we infer that the incorporation of alkali earth metal with lower electronegativity than magnesium in MOF-74 is likely to affords an opportunity to enhance the electron density of phenolate oxygen in order to study their impact on the basicity and related catalytic activity in Knoevenagel condensation.

Currently, there is no report regarding to the one-pot synthesis of alkaline earth MOF-74 other than Mg-MOF-74. Attempts to prepare these alkaline earth MOF-74 directly by the reaction of alkaline earth metal salts with 2,5-dihydroxyterephthalate were unsuccessful. Post-synthetic cation exchange is a well-known approach to bring exogenous metals into MOFs' MBBs without damaging the structure.[15] Nevertheless, the reported exchange processes often occur between two transition metals owing to the similarity of electronic arrangement.[16] We herein demonstrate for the first time that Zn-MOF-74 can be subjected to post-synthetic alkaline earth metal exchange. The resulting Ca/Zn-MOF-74 exhibits enhanced basicity and catalytic activity in the Knoevenagel condensation.

Zn-MOF-74 was immersed in a DMF solution of $CaCl_2$. Color of Zn-MOF-74 changed from light yellow to brown during the exchange. The exchange process at different temperatures (25-100 °C) is traced by inductively coupled plasma atomic emission spectrometer (ICP-AES), from which the quantity of Ca^{2+} in solid is consistent with Zn^{2+} in the exchange reaction solution (Fig. 1a-b). Zn-MOF-74 is partially exchanged with Ca^{2+}

---

[a] State Key Laboratory of Materials-Oriented Chemical Engineering, College of Chemical Engineering, Nanjing Tech University, No. 30 Puzhunan Road, Nanjing 211816, China.
[b] Jiangsu National Synergetic Innovation Centre for Advanced Materials (SICAM), No. 5 Xinmofan Road, Nanjing 210009, China.

Electronic Supplementary Information (ESI) *available: Experimental section,* elemental mapping, EDX spectrum, TG analysis, CO_2-TPD analysis, XRD *patterns,* Rietveld refinement, N_2 sorption isotherms. *See DOI: 10.1039/x0xx00000x*

View Article Online
DOI: 10.1039/C9DT03332G

after 7 days at 75 °C (33%), however, only 20% of Zn^{2+} in MOF-74 was exchanged when temperature is reduced to 50 °C. Increasing the exchange temperature to 100 °C results in a high exchange ratio of 68%, but the microporous structure is likely to be damaged as indicated by the presence of mesopores according to pore size analysis (Fig. 1c). Thermogravimetric analysis in O_2 atmosphere verifies that the molar ratios of CaO:ZnO in Ca/Zn-MOF-74 (25-75 °C) are consistent with the ICP-AES result except for Ca/Zn-MOF-74 (100 °C) (see the ESI for details). From SEM images of Ca/Zn-MOF-74 (25-100 °C) (Fig. 1d), there is no significant change on morphology other than the sample exchanged at 100 °C. The particle surface of Ca/Zn-MOF-74 (100 °C) became irregular with coarse surface indicating the partial collapse of MOF structure which is consistent with its pore size distribution and mismatch between results of TGA and ICP-AES. Given both exchange progress and the stability of the pore structure, we decided to choose Ca/Zn-MOF-74 exchanged at 75 °C for subsequent studies and all the Ca/Zn-MOF-74 mentioned later specifically refers to the sample exchanged at 75 °C for 7 days.

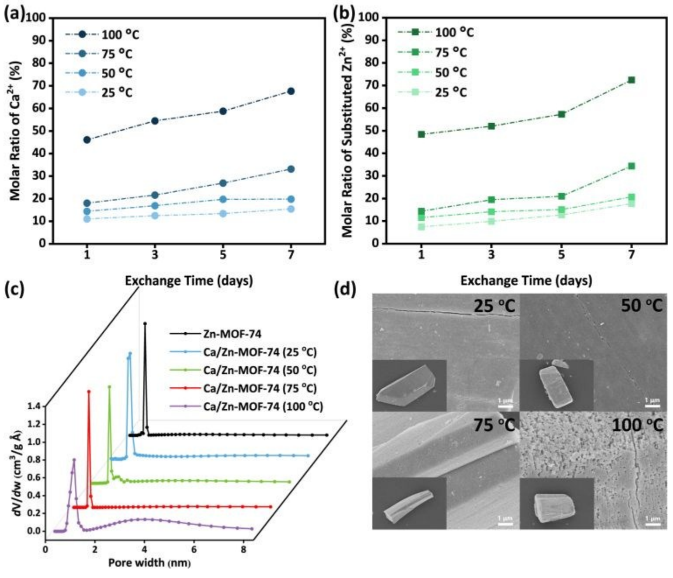

Fig. 1 (a) Molar ratio of Ca:(Ca+Zn) in Ca/Zn-MOF-74; (b) Molar ratio of Zn (substituted):Zn (total) according to Zn^{2+} concentration in the solution after exchange; (c) NLDFT pore size distribution of Zn-MOF-74 and Ca/Zn-MOF-74; (d) SEM images of morphology of Ca/Zn-MOF-74 at 25-100 °C. (insets pictures are corresponding particle of Ca/Zn-MOF-74 exchanged at 25-100 °C)

Powder X-ray diffraction (PXRD) pattern of Ca/Zn-MOF-74 is comparable to the parent Zn-MOF-74, and we found a slight shift of diffraction peak from 2θ value of 7.0° to 6.8° after the exchange process (Fig. 2a). This phenomenon can be attributed to the metathesis of smaller Zn^{2+} by larger Ca^{2+}, giving rise to the expansion of interplanar distance of (2-10) planes and corresponding slight increase of the BET surface area (from 688 to 758 m^2/g) (Fig. 2b). The structure expansion is confirmed by Rietveld refinement of PXRD data. Ca/Zn-MOF-74 crystallized in *R-3* with a = b = 26.0556(82), c = 6.8505(23), which is slightly higher than cell parameters of parent Zn-MOF-74 (a = b = 25.9322(15), c = 6.8365(4)), presumably because of the longer Ca-O distance (average 2.096 Å). Time-of-flight mass spectrometry (TOFMS) of Ca/Zn-MOF-74 shows a new signal of calcium cations in the positive spectra (Fig. 2c), and there was no signal of chloride anions in the negative ion spectra (Fig. 2d). It can be inferred that calcium cations indeed substitute zinc cations in Zn-MOF-74 rather than reside within the channels of Zn-MOF-74 as chlorine salt. Uniform distribution of Ca^{2+} in Ca/Zn-MOF-74 is confirmed by EDX spectrum, in which both Ca^{2+} and Zn^{2+} are highly dispersed in both exterior and internal surfaces of the crystalline particles (Fig. S7). Thermogravimetric analysis in N_2 atmosphere (Fig. S8) reveals that Ca/Zn-MOF-74 and Zn-MOF-74 exhibit a similar thermal stability with 22.8% and 17.7% weight loss, respectively, from 30 °C to 200 °C. These weight losses correspond to the loss of DMF, methanol and H_2O, and followed by a steady plateau from 200 °C to 410 °C and 400 °C respectively, before decomposition.

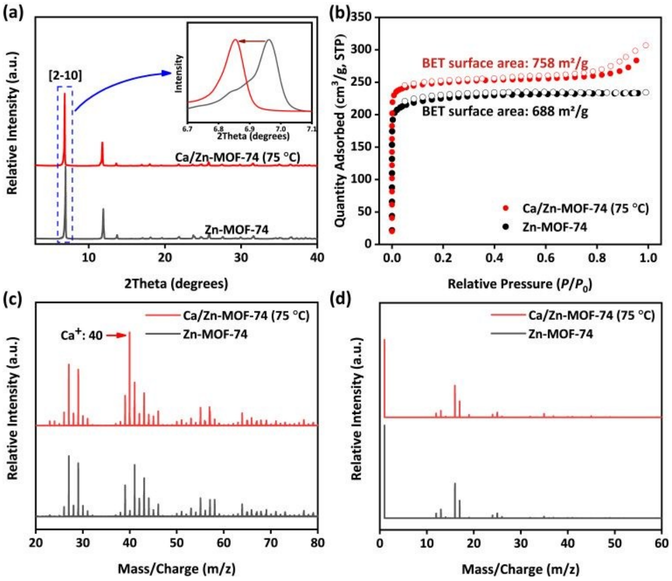

Fig. 2 (a) PXRD patterns, (b) N_2 sorption isotherms at 77 K, (c) TOFMS positive ions spectra and (d) TOFMS negative ions spectra of Zn-MOF-74 and Ca/Zn-MOF-74.

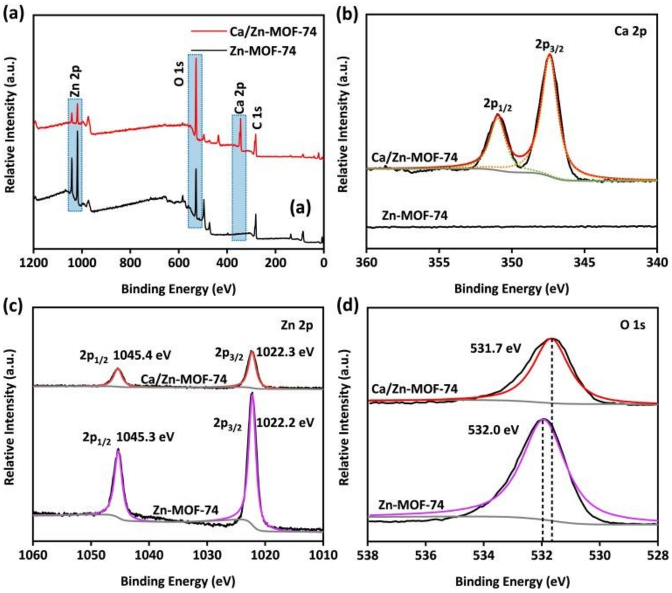

Fig. 3 XPS spectra of Zn-MOF-74 and Ca/Zn-MOF-74: (a) survey spectrum; (b) Ca 2p spectra; (c) Zn 2p spectra; (d) O 1s spectra.

DOI: 10.1039/C9DT03332G

The chemical composition of Ca/Zn-MOF-74 were furtherly studied by X-ray photoelectron spectroscopy (XPS). Three main peaks are observed at 284.4, 532.0 and 1022.2 eV in the XPS spectrum of Zn-MOF-74, which are ascribed to C 1s, O 1s and Zn 2p respectively (Fig. 3a). After Ca^{2+} exchange, two new peaks appear at 350.9 and 347.4 eV corresponding to Ca $2p_{1/2}$ and Ca $2p_{3/2}$, which indicates the incorporation of Ca^{2+} (Fig. 3b). With the appearance of Ca 2p signals, the peak intensities of $Zn_{1/2}$ and $Zn_{3/2}$ decrease significantly (Fig. 3c). This phenomenon is consistent with the ICP results, indicating that the Zn^{2+} in the MOF structure are partially substituted by Ca^{2+}. It is worth noting that there is a negative shift of binding energy of O 1s spectra from 532.0 to 531.7 eV after exchange (Fig. 3d). This shift indicates an increase in electron density around oxygen atoms due to the lower electron affinity of Ca^{2+}.[17] The increase of the electron density in turn improve the proton affinity of oxygen, which offers the chance for enhanced the basicity of Ca/Zn-MOF-74.

MOF-74 has two kinds of basic sites arising from coordination unsaturated phenolate oxygen atoms and carboxylate oxygen atoms.[13] According to Sanderson's theory of electronegativity[18], Ca^{2+} substituted Zn-MOF-74 is supposed to exhibit enhanced basicity due to the lower electronegativity of calcium. To verify our hypothesis, CO_2-TPD was used to evaluate the basic strength of the material before and after cation exchange (Fig. S9). Taking the thermal stability into account, TPD temperature is only set to 400 °C. Two broad desorption peaks of Ca/Zn-MOF-74 at approximately 125 °C and 380 °C, which are higher than Zn-MOF-74 (110 °C and 367 °C), are attributed to weak and medium basic sites generated from carboxylate oxygen atoms and phenolate oxygen atoms. The difference on desorption temperature indicates the enhanced basicity of Ca/Zn-MOF-74, which is in good agreement with the results of XPS.

The catalytic activities of Ca/Zn-MOF-74 for the Knoevenagel condensation, a classic reaction catalyzed by base, was evaluated. Different benzaldehyde derivatives were used with malononitrile under the same condition. The catalytic results of Knoevenagel condensation reactions are shown in Table 1. When Ca/Zn-MOF-74 was used as catalyst, the reaction of benzaldehyde with malononitrile gave a high yield of 88%, which was twice of the parent Zn-MOF-74. The effect of substituent groups on benzaldehyde were investigated as shown in entry 2-6. It is clear that the reaction of benzaldehyde with electron-withdrawing groups (e.g. $-NO_2$, -CN, -Cl) gives a higher yield of the product than benzaldehyde with electron-donating groups such as $-CH_3$ and $-C_2H_5$. In order to further explore the effect of Ca^{2+} on the catalytic activity of Ca/Zn-MOF-74, we also synthesized Ni^{2+}-exchanged Ni/Zn-MOF-74, of which the exchange ratio (48%) is even larger than Ca/Zn-MOF-74 (33%). In the MOF-74 family, Ni-MOF-74 exhibits the best base catalytic activity. However, Ca/Zn-MOF-74 exhibits much higher yield than Ni/Zn-MOF-74 for all benzaldehyde derivatives. The higher catalytic activity for Ca/Zn-MOF-74 compared with Ni/Zn-MOF-74 could be presumably attributed to the stronger proton affinity of structural phenolate oxygen in Ca/Zn-MOF-74, which facilitate the activation of donor molecules, followed by the attack of benzaldehyde.

Table 1 Catalytic properties of Ca/Zn-MOF-74 in the Knoevenagel condensation

Reaction condition: aldehyde (1 mmol), malononitrile (1 mmol), catalyst (50 mg), toluene (2 mL), temp.: 70 °C, time: 12h. [a] Zn-MOF-74 as catalyst. [b] Ni/Zn-MOF-74 as catalyst. [c] Ca/Zn-MOF-74 as catalyst.

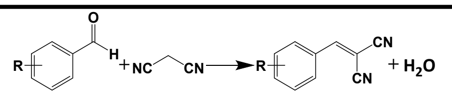

Entry	Aldehyde	product	Yield[a] (%)	Yield[b] (%)	Yield[c] (%)
1	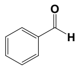	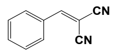	42	55	88
2	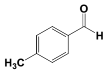	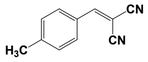	31	49	82
3	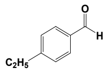	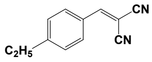	24	30	74
4	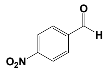	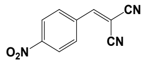	47	61	93
5	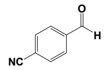	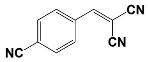	46	53	90
6	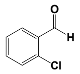	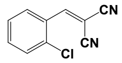	60	65	96

In summary, we have successfully synthesized a rare Ca/Zn-MOF-74 via post-synthetic Ca^{2+} exchange of Zn-MOF-74. The exchange process is monitored by ICP-AES and the resulting Ca/Zn-MOF-74 exhibits permanent porosity that is comparable to the parent Zn-MOF-74. The enhanced basicity of Ca/Zn-MOF-74 is confirmed by XPS and CO_2-TPD. The catalytic property of Ca/Zn-MOF-74 are highly desirable in that they maximise the product yield compared to parent Zn-MOF-74 and Ni/Zn-MOF-74 in the context of Knoevenagel condensations. The promising features of Ca/Zn-MOF-74 indicate that alkaline metal-incorporated MOF-74 can serve as platforms for the generation of MOF with intrinsic basicity that would otherwise be impossible to realize.

We would acknowledge National Key R&D Program of China (2017YFB0307304), National Natural Science Foundation of China (21676141, 21808104), Natural Science Foundation of Jiangsu Province (BK20170989) and Natural Science Foundation of Jiangsu Higher Education Institutions of China (17KJB530005). The authors are grateful for the helpful discussions and advices given by Prof. Dr. D. Yang.

Conflicts of interest

There are no conflicts to declare.

Notes and references

1 (a) S. Batten, S. Neville and D. Turner, *Coordination Polymers: Design, Analysis and Application*, Royal Society of Chemistry, Cambridge, UK, 2009; (b) L. R. MacGillivray, *Metal-Organic Frameworks: Design and Application*, John Wiley & Sons, Hoboken, 2010.

View Article Online
DOI: 10.1039/C9DT03332G

2 (a) B. Moulton and M. J. Zaworotko, *Chem. Rev.*, 2001, **101**, 1629-1658. (b) G. R. Desiraju, *Crystal Engineering: The Design of Organic Solids*, Elsevier, Amsterdam,1989.

3 (a) S. Abednatanzi, P. Gohari Derakhshandeh, H. Depauw, F. X. Coudert, H. Vrielinck, P. Van Der Voort and K. Leus, *Chem. Soc. Rev.*, 2019, **48**, 2535-2565; (b) J. J. Perry, J. A. Perman and M. J. Zaworotko, *Chem. Soc. Rev.*, 2009, **38**, 1400-1417.

4 (a) Z. Wang and S. M. Cohen, *Chem. Soc. Rev.*, 2009, **38**, 1315-1329; (b) C. K. Brozek and M. Dinca, *Chem. Soc. Rev.*, 2014, **43**, 5456-5467.

5 (a) J. Lee, O. K. Farha, J. Roberts, K. A. Scheidt, S. T. Nguyen and J. T. Hupp, *Chem. Soc. Rev.*, 2009, **38**, 1450-1459; (b) T. Zhang and W. Lin, *Chem. Soc. Rev.*, 2014, **43**, 5982-5993.

6 J. S. Seo, D. Whang, H. Lee, S. I. Jun, J. Oh, and Y. Jin, and K. Kim, *Nature*, 2000, **404**, 982–986.

7 M. Fujita, Y. J. Kwon, S. Washizu and K. Ogura, *J. Am. Chem. Soc.*, 1994, **116**, 1151-1152.

8 (a) P. Ji, T. Drake, A. Murakami, P. Oliveres, J. H. Skone and W. Lin, *J. Am. Chem. Soc.*, 2018, **140**, 10553-10561; (b) D. Yang, M. A. Ortuno, V. Bernales, C. J. Cramer, L. Gagliardi and B. C. Gates, *J. Am. Chem. Soc.*, 2018, **140**, 3751-3759; (c) Y.-Z. Li, H.-H. Wang, H.-Y. Yang, L. Hou, Y.-Y. Wang and Z. Zhu, *Chem. Eur. J.*, 2018, **24**, 865-871; (d) H.-H. Wang, L. Hou, Y.-Z. Li, C.-Y. Jiang, Y.-Y. Wang and Z. Zhu, *ACS Appl. Mater. Interfaces,* 2017, **9**, 17969-17976.

9 (a) A. Dhakshinamoorthy, A. M. Asiri and H. Garcia, *Angew. Chem. Int. Ed.*, 2016, **55**, 5414-5445; (b) N. Kornienko, Y. Zhao, C. S. Kley, C. Zhu, D. Kim, S. Lin, C. J. Chang, O. M. Yaghi and P. Yang, *J. Am. Chem. Soc.*, 2015, **137**, 14129-14135; (c) S. R. Ahrenholtz, C. C. Epley and A. J. Morris, *J. Am. Chem. Soc.*, 2014, **136**, 2464-2472.

10 L. B. Sun, X. Q. Liu and H. C. Zhou, *Chem. Soc. Rev.*, 2015, **44**, 5092-5147.

11 (a) P. Valvekens, D. Jonckheere, T. De Baerdemaeker, A. V. Kubarev, M. Vandichel, K. Hemelsoet, M. Waroquier, V. Van Speybroeck, E. Smolders, D. Depla, M. B. J. Roeffaers and D. De Vos, *Chem. Sci.*, 2014, **5**, 4517-4524; (b) R. Sen, D. Saha and S. Koner, *Chem. Eur. J.*, 2012, **18**, 5979-5986.

12 H. Hattori, *Appl. Catal. A: Gen.*, 2015, **504**, 103-109.

13 P. Valvekens, M. Vandichel, M. Waroquier, V. Van Speybroeck and D. De Vos, *J. Catal.*, 2014, **317**, 1-10.

14 B. M. Choudary, M. L. Kantam, V. Neeraja, K. K. Rao, F. Figueras and L. Delmotte, *Green Chem.*, 2001, **3**, 257-260.

15 M. Lalonde, W. Bury, O. Karagiaridi, Z. Brown, J. T. Hupp and O. K. Farha, *J. Mater. Chem. A*, 2013, **1**, 5453-5468.

16 (a) C. K. Brozek and M. Dinca, *J. Am. Chem. Soc.*, 2013, **135**, 12886-12891; (b) R. J. Comito, K. J. Fritzsching, B. J. Sundell, K. Schmidt-Rohr and M. Dinca, *J. Am. Chem. Soc.*, 2016, **138**, 10232-10237; (c) S. Canossa, L. Fornasari, N. Demitri, M. Mattarozzi, D. Choquesillo-Lazarte, P. Pelagatti and A. Bacchi, *CrystEngComm*, 2019, **21**, 827-834.

17 (a) R. G. Pearson, *Inorg. Chem.*, 1988, **27**, 734-740; (b) Y. C. Tan and H. C. Zeng, *Nat. Commun.*, 2018, **9**.

18 R. T. Sanderson, *Inorg. Chem.*, 1986, **25**, 3518-3522.1.